Nuclear Engineering and Technology 53 (2021) 1955–1963

Contents lists available at ScienceDirect

Nuclear Engineering and Technology

journal homepage: www.elsevier.com/locate/net

Original Article

Investigation of a novel on-site U concentration analysis method for UO_2 pellets using gamma spectroscopy

Haneol Lee*, Chan Jong Park

Korea Institute of Nuclear Non-proliferation and Control (KINAC), 1418 Yuseong-daero, Yuseong-gu, Daejeon, 34101, Republic of Korea

ARTICLE INFO

Article history:
Received 13 July 2020
Received in revised form
29 November 2020
Accepted 30 November 2020
Available online 4 December 2020

Keywords:
On-site U concentration verification
Nuclear safeguards
Characteristic X-ray
National inspection
Gamma spectroscopy

ABSTRACT

As the IAEA has applied integrated safeguards and a state level approach to member states, the importance of national inspection has increased. However, the requirements for national inspection for some member states are different from the IAEA safeguards. In particular, the national inspection for the ROK requires on-site U concentration analysis due to a domestic notification. This research proposes an on-site U concentration analysis (OUCA) method for UO_2 pellets using gamma spectroscopy to satisfy the domestic notification requirement. The OUCA method calculates the U concentration of UO_2 pellets using the measured net X-ray counts and declared ^{235}U enrichment. This research demonstrates the feasibility of the OUCA method using both MCNP simulation and experiment. It simulated and measured the net X-ray counts of different UO_2 pellets with different U concentrations and ^{235}U enrichments. The simulated and measured net X-ray counts were fitted to polynomials as a function of U concentration and ^{235}U enrichment. The goodness-of-fit results of both simulation and experiment demonstrated the feasibility of the OUCA method.

1. Introduction

The International Atomic Energy Agency (IAEA) defines nuclear safeguards as “the timely detection of diversion of nuclear material from peaceful nuclear activities to the manufacture of nuclear weapons or of other nuclear explosive devices …” [1]. Nuclear materials which are subjected to the IAEA safeguards are defined as special nuclear material (SNM). The member states of the IAEA have government agencies which account for domestic SNM. The government agencies perform an independent national inspection. The importance of national inspection increases as the IAEA implements integrated safeguards (IS) and a state level approach (SLA) to member states.

The IAEA applied integrated safeguards to the Republic of Korea (ROK) in July 2008. The ROK, as a member state of IAEA, is obligated to control domestic SNMs based on a state system of accounting and control (SSAC) [2]. The Korea Institute of Nuclear non-proliferation and Control (KINAC) is committed to the control of domestic SNM by the Nuclear Safety and Security Council (NSSC). KINAC has to perform national inspection based on the “article 4 of the NSSC notification (2017–83)” [3]. The domestic notification requires the inspectors of national inspection to verify the composition as well as total amount of SNM in nuclear facilities.

The IAEA verifies the amount of SNMs in a facility using a sampling based approach since verifying all SNMs in a facility is almost impossible. The IAEA classifies the level of verification into three defect types (gross, partial and bias defect) and calculates the corresponding sample size for each verification level. Table 1 describes the definition and characteristics of the three different defect types [4].

The IAEA calculates the amount of SNM by multiplying the net weight, the concentration of the SNM (U, Pu factor), and the isotope fraction (enrichment) of the SNM. For gross defect verification, the IAEA only verifies whether the material exists as declared. For partial defect verification, the IAEA calculates the amount of SNM using both on-site measurement results (net weight, SNM enrichment) and operator declared results (SNM concentration). For bias defect verification, the IAEA calculates the amount of SNM using the results from laboratory analyses. The conventional three-step process does not conflict with the purpose of IAEA’s SNM verification since its only goal is to verify the amount of SNM. However, it becomes a problem for the national inspection of some member states, such as the ROK.

Conventional IAEA sampling cannot be applied to the ROK directly for partial defect verification, due to the IAEA’s use of

* Corresponding author.
E-mail address: haneol@kinac.re.kr (H. Lee).

https://doi.org/10.1016/j.net.2020.11.030

Table 1
Characteristics of different defect types.

Defect type	Definition	Target of verification	Location of verification	Methods used
Gross defect	Entire material being missing or diverted	Material type	On-site	Gamma spectroscopy
Partial defect	Some fraction (less than 50%) of material being missing or diverted	Amount of SNM	On-site	Weighting, Gamma spectroscopy
Bias defect	Small amount (bias level) of material being missing or diverted	Amount of SNM	Analysis Laboratory	Chemical Analysis

"operator declared SNM concentration", which is a characteristic that needs to be verified in the national inspection. Two possible solutions exist to overcome the problem. The first solution is to design an independent sampling method for national inspection. The second solution is to suggest an on-site SNM concentration analysis method.

This research adopted the second solution to minimize the additional burden and sampling difference between the IAEA and a member state, in this case, the ROK. The goal of this research was to suggest a method which analyzes the U concentration of UO_2 pellets using gamma spectroscopy. The target was limited to UO_2 pellets to demonstrate the feasibility of the method. This research demonstrated the feasibility of the method using a computational model and also performed validation experiments using different UO_2 pellets with different ^{235}U enrichments and U concentrations.

1.1. Methods of U concentration analysis

A number of methods has been developed and applied for U concentration analysis of nuclear materials. An IAEA technical report (IAEA/NVS/1) summarized the conventional methods [5]. Titration, coulometry, thermogravimetric analysis, and X-ray fluorescence methods have been widely used to analyze the U concentration of UO_2 pellets. Titration, coulometry, and thermogravimetric methods are destructive assays (DAs), and X-ray fluorescence (XRF) is a non-destructive assay (NDA). The characteristics of each method are described in Table 2 [6–10].

Table 2 indicates that the existing methods have limitations in measuring the U concentration of UO_2 pellets for partial defect verification. DA based methods (titration, coulometry and thermogravimetric analysis) cannot be applied on site, while the high relative uncertainty of XRF makes it appropriate for qualitative rather than quantitative analysis. The goal of this research was to suggest an on-site U concentration analysis method for partial defect verification which can overcome the limitations of the methods in Table 2.

UO_2 pellets emit gamma rays in a wide energy range due to the radioactive decay of ^{235}U, ^{238}U and their daughter nuclides. Gamma rays interact with the electrons of uranium atoms in a pellet and generate the characteristic X-rays of uranium. If the ^{235}U enrichment and geometry of UO_2 pellets are consistent, the intensity of uranium's characteristic X-ray will be proportional to the U concentration of a pellet. This research assumed that the ^{235}U enrichment in a pellet was measured before the U concentration measurement.

The on-site U concentration analysis method measures the net count of uranium's characteristic X-ray in the K_α energy region (92–100 keV) and K_β energy region (112–115 keV) using a gamma detector. It then calculates the net X-ray counts by eliminating gamma peaks from the net count of the energy region. The net count of overlapped gamma peaks is calculated using the emission yield, the ^{235}U enrichment, and the net count of the 185.7 keV peak. This research named the U concentration analysis method using gamma spectroscopy as "On-site Uranium Concentration Analysis (OUCA)". The detailed process to calculate U concentration using the OUCA method is described below.

This research defined C_1, C_2, and C_3 as the net counts for the K_α energy region, K_β energy region, and 185.7 keV gamma peak. The net count of the 185.7 keV peak is calculated using equation (1). The net count of gamma peaks from ^{235}U, ^{238}U, and their daughter nuclides were then calculated using equations (2) and (3). Due to the secular equilibrium, the activity of daughter nuclides (^{231}Pa, ^{231}Th, ^{234m}Pa, ^{234}Th) which affects the net counts (C_1 and C_2) is consistent with their parent nuclides (^{235}U, ^{238}U). This research neglected ^{236}U inside a pellet and gamma peaks with an emission yield smaller than 10^{-3}.

$$C_3 = A_{eff}(235U)Y(185.7)\varepsilon(185.7)\varepsilon_{others} \quad (1)$$

$$C_{\gamma,235} = C_3\frac{\sum_i^{N_i} Y(E_i)\varepsilon(E_i)}{Y(185.7)\varepsilon(185.7)} \quad (2)$$

$$C_{\gamma,238} = C_3\frac{(1-w)\lambda_{238}}{w\lambda_{235}}\frac{\sum_j^{N_j} Y(E_j)\varepsilon(E_j)}{Y(185.7)\varepsilon(185.7)} \quad (3)$$

where.

$A_{eff}(^{235}U)$: Effective activity of ^{235}U in a pellet ($= \lambda_{235} wf N_U$).

Table 2
Characteristics of conventional methods for U concentration analysis.

Methods	Procedure	Characteristics	$u_{rel.}$ (%)
Titration	- Dissolve sample into acid - Reduce U(VI) into U(IV) using Fe^{2+} - Oxidize U(IV) into U(IV) using $K_2Cr_2O_7$ - Calculate U concentration using the amount of $K_2Cr_2O_7$ used to the end point	- DA - Target: U/Pu compounds - Sample preparation	0.07
Coulometry	- Dissolve sample into acid - Pre-electrolyze the dissolved sample - Oxidize/reduce the sample under electric potential until residual current disappears - Calculate U concentration using the amount of charge used for equilibrium	- DA - Target: U/Pu compounds - Sample preparation	0.04(U), 0.14(Pu)
Thermo-gravimeteric	- Ignite the sample under oxidizing/reducing atmosphere - Calculate U concentration using the mass change before and after ignition	- DA - Target: U/Pu oxides - No sample preparation	0.07
X-ray fluorescence	- Irradiate sample with X-ray - Measure the intensity of characteristic X-ray - Calculate U concentration using the intensity	- NDA - Target: U/Pu compounds	~10

λ_{235}: Decay constant of ^{235}U, λ_{238}: Decay constant of ^{238}U.
w: Enrichment of ^{235}U.
f: Active fraction of a pellet, N_U: Number of U in a pellet.
$Y(185.7)$: Yield of 185.7 keV peak emission from ^{235}U.
$\varepsilon(185.7)$: Energy efficiency of the detector at 185.7 keV.
ε_{others}: Other efficiencies of the detector.
$C_{\gamma,235}$: Net count of gamma peaks from ^{235}U and its daughter nuclides within energy range.
$C_{\gamma,238}$: Net count of gamma peaks from ^{238}U and its daughter nuclides within energy range.
N_i: Number of gamma peaks from ^{235}U and its daughter nuclides within energy range.
N_j: Number of gamma peaks from ^{238}U and its daughter nuclides within energy range.

The net count of uranium's K_α and K_β X-ray is then calculated by subtracting the calculated counts of gamma peaks ($C_{\gamma,235}$ and $C_{\gamma,238}$) from the net counts (C_1 and C_2), as described in equations (4) and (5). Since the characteristic X-ray is generated by the interaction between gamma rays and the orbital electron of an atom, the net count of uranium's characteristic X-ray is affected by its atomic density and gamma ray intensity. Uranium's atomic density and gamma ray intensity are proportional to the U concentration and ^{235}U enrichment, respectively. As a result, the net count of the K_α or K_β X-ray is expressed as a function of U concentration and then fitted to a second order polynomial (equation (6)). The overall process of the OUCA method is depicted in Fig. 1.

$$C_{\alpha,ROI} = C_1 - C_{\gamma,235} - C_{\gamma,238} \tag{4}$$

$$C_{\beta,ROI} = C_2 - C_{\gamma,235} - C_{\gamma,238} \tag{5}$$

$$C_{\alpha/\beta,ROI}(w, f_U) = \left(Af_U^2 + Bf_U + C\right)\left(Dw^2 + Ew + F\right) \tag{6}$$

where.
$C_{\alpha,ROI}$: Net count of uranium's K_α X-ray in the energy region.
$C_{\beta,ROI}$: Net count of uranium's K_β X-ray in the energy region.
$C_{\alpha/\beta,ROI}$: Net count of uranium's K_α or K_β X-ray in the energy region.
f_U: U concentration in a pellet.
w: ^{235}U enrichment of a pellet.
A, B, C, D, E, F: Constants.

1.2. Simulation based feasibility demonstration

To demonstrate the feasibility of the OUCA method, this research performed a computational simulation due to the limited access on pellets with consistent geometry, different ^{235}U enrichment, and different U concentration. This research simulated an HPGe gamma ray detector using the MCNPX code. The diameter and height of the UO_2 pellets used for simulation were 0.8190 and 1 cm, respectively. The density of the simulated pellets was 95% of theoretical density (TD) of UO_2. The simulated pellets had four different U concentrations by applying some fraction of burnable poison (88.15 (Pure), 84.62 (4 wt% Gd_2O_3), 82.86 (6 wt% Gd_2O_3), 81.90 (8 wt% Gd_2O_3) %U) and seven different ^{235}U enrichments (1.5, 2.0, 2.5, 3.0, 3.5, 4.0, 4.5 wt%).

This research initially simulated the net count of uranium's characteristic X-ray using the MCNPX code by subtracting the gamma peaks from the net count of the ROI. The simulated results were then normalized with U concentration to demonstrate the polynomial in equation (6) whose parameter is ^{235}U enrichment. The simulated results were also normalized with ^{235}U enrichment to demonstrate the polynomial in equation (6) whose parameter is U concentration. The goodness-of-fit of the polynomials was demonstrated using the R^2 method. This research then derived equation (6) to demonstrate the feasibility of the OUCA method using the fitted polynomials and a reference pellet.

This research simulated the feasibility of the OUCA method using an n-type coaxial HPGe detector (ORTEC GMX60P4), which is a main detector for Compton suppression system in the KINAC. It suppresses the Compton continuum by eliminating coincidence counts using a main (HPGe) detector and several auxiliary (NaI(Tl)) detectors. The geometry and specifications of the HPGe detector are described in Fig. 2 and Table 3. Since the OUCA method only used the HPGe detector, the auxiliary NaI(Tl) detectors were not simulated in this research. The computational model simulated the gamma spectrum inside the detector using the pulse height tally (F8 tally) of the MCNPX code. The Gaussian energy broadening (GEB) function was applied using equation (7) to simulate the FWHM of each peak [11]. This research considered both photon and electron simulation. The 10 keV electron energy cutoff was applied to reduce the simulation time. It simulated 10^8 particles to maintain the relative uncertainty, at each X-ray and gamma peak energy bin, at less than 0.05.

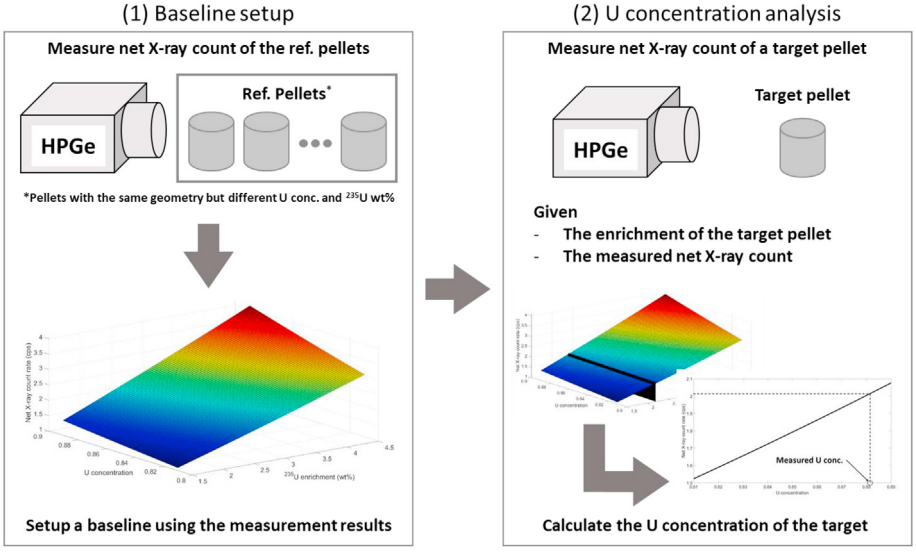

Fig. 1. A schematic diagram of the OUCA method.

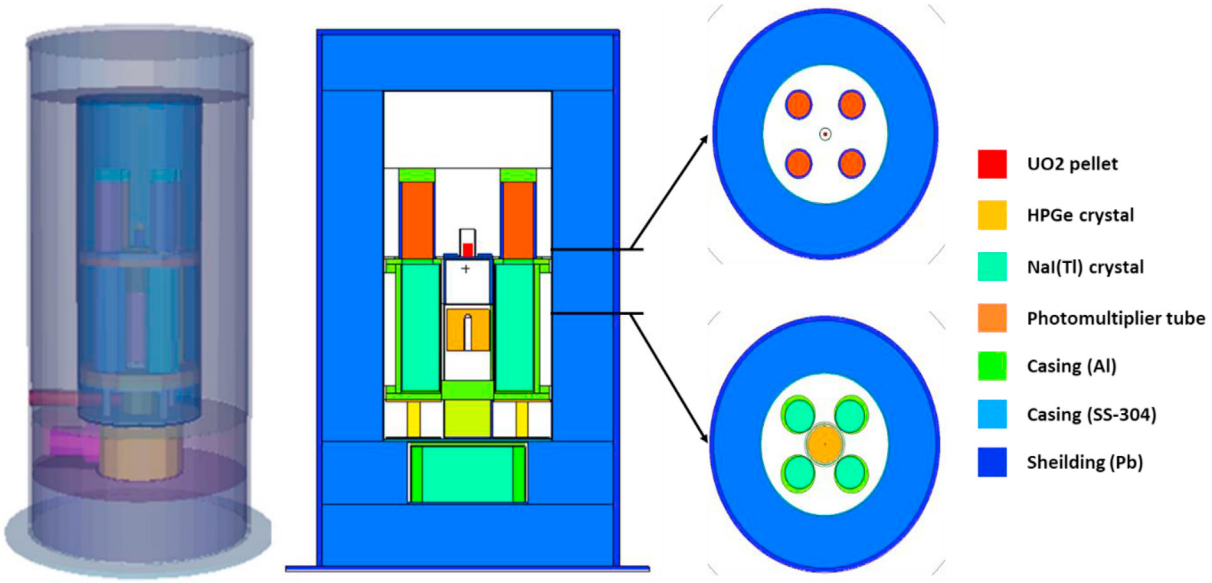

Fig. 2. Geometry of gamma ray detector used for simulation.

Table 3
Specifications of an n-type HPGe detector used for simulation.

	Characteristics
Crystal size	(OD) 7.188 cm, (height) 7.526 cm
Rel. efficiency	60%
FWHM	2.3 keV at 1330 keV
Collimator	No

$$FWHM(E) = a + b\sqrt{E + cE^2} \quad (7)$$

where.

$FWHM(E)$: Full width half maximum at energy E (MeV).

E: Energy of X-ray and gamma peaks (MeV).

a: Constant ($a = 9.60 \times 10^{-4}$ for the simulated detector),

b: Constant ($b = 1.20 \times 10^{-4}$ for the simulated detector).

c: Constant ($c = 7.03 \times 10^{2}$ for the simulated detector).

The MCNPX simulation requires the relative gamma intensity as a source card. This research calculated the gamma source distribution of a pellet using the OrigenArp code [12] and KAERI's nuclear database [13]. The OrigenArp code calculated the mass of the radionuclides per unit mass. The intensity of gamma peaks was calculated using the gamma emission yield of the nuclear database. This research made the following assumptions to minimize the "age effect" of UO_2 pellets, generated by the composition of daughter nuclides, on calculating the intensity of gamma peaks.

Daughter nuclides of ^{235}U and ^{238}U are separated during the fuel fabrication process.

Pellets with one year after manufacture are used for simulation.

Gamma photons are only emitted by uranium and its daughter nuclides.

Based on the assumptions, this research defined the major nuclide as uranium isotopes (^{234}U, ^{235}U, and ^{238}U) and daughter nuclides with secular equilibrium. Then the major nuclides in a UO_2 pellet become ^{234}U, ^{235}U, ^{238}U, ^{231}Pa, ^{234m}Pa, ^{230}Th, ^{231}Th, and ^{234}Th. This research also defined effective gamma peak as a gamma peak whose emission yield is larger than 10^{-4}, based on the nuclear database. The calculated gamma peaks were then normalized to have a normalized intensity. Fig. 3 depicts the relative intensity of gamma peaks for a pellet with 88.15% U concentration and 4.5 wt% ^{235}U enrichment. Characteristics of 10 gamma peaks with high relative intensity are summarized in Table 4. The relative intensity of gamma peaks for the other pellets was also calculated. This research then simulated 28 UO_2 pellets to calculate the relative pulse height in the detector crystal.

The calculated relative pulse height for 28 pellets were then processed using the sensitive non-linear iterative peak (SNIP) method [14]. This research defined the results of MCNPX simulation as a relative count (count per initial gamma particle). The relative count of the K_α energy region (C_1), K_β energy region (C_2), and 185.7 keV gamma peak (C_3) were then calculated using the processed simulation results. Fig. 4 depicts the simulated gamma spectrum using the HPGe detector and pellet with 88.15% U concentration and 4.5 wt% ^{235}U enrichment.

Since the net relative count of K_α and K_β X-rays is calculated using equations (4) and (5), the relative energy efficiency of gamma

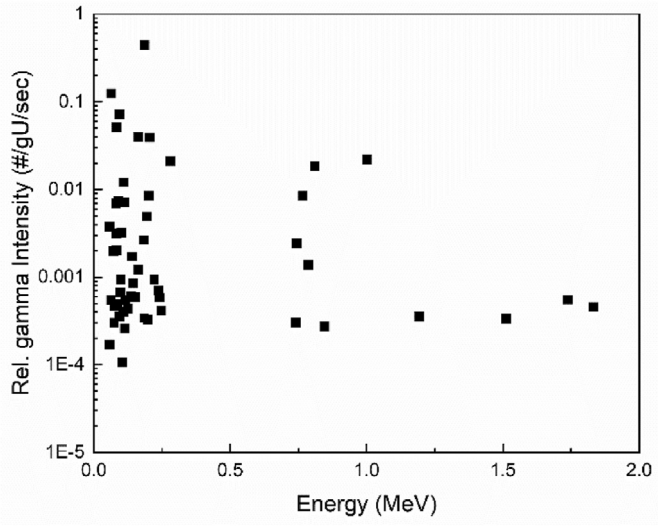

Fig. 3. Relative intensity of major gamma peaks in a pellet (88.15% U concentration, 4.5 wt% ^{235}U enrichment).

Table 4
Characteristics of gamma peaks with high relative intensity.

Peak energy (keV)	Emission yield (%)	Source
63.29	12.48	^{234}Th
84.21	5.157	^{231}Th
92.38	7.252	^{234}Th
92.80	7.148	^{234}Th
163.3	3.939	^{235}U
185.7	44.69	^{235}U
205.3	3.915	^{235}U
279.5	2.110	^{235}U
810.3	1.857	^{234}Th
1001	2.207	^{234m}Pa

peaks in the X-ray energy range and 185.7 keV has to be calculated. The energy efficiency at each gamma peak was calculated by dividing the simulated count by the relative source intensity (equation (8)). The UO_2 pellet used for energy efficiency calculation was the same pellet used for the feasibility demonstration. The energy efficiency curve was then calculated by fitting the simulated relative energy efficiency at gamma peaks into a polynomial (equation (9)). The selected gamma peaks, with high relative intensity, were the gamma peaks in Table 4. It also selected gamma peaks which do not overlap with any other peaks. The simulated efficiency for gamma peaks and the calculated efficiency curve are depicted in Fig. 5. The results in Fig. 5 indicate that the efficiency of low energy gamma peaks was suppressed due to the self-attenuation inside high density source material (UO_2, 10.41 g/cm^3).

$$\varepsilon(E_i) = C(E_i)/S(E_i) \tag{8}$$

$$\ln(\varepsilon(E_i)) = a\ln(E_i)^5 + b\ln(E_i)^4 + c\ln(E_i)^3 + d\ln(E_i)^2 + e\ln(E_i) + f \tag{9}$$

where.

$\varepsilon(E_i)$: Energy efficiency at E_i,

$C(E_i)$: Simulated net relative count at E_i, $S(E_i)$: Relative source intensity at E_i,

a: Constant (a = 0.56300 for the simulated detector), b: Constant (b = 3.5436 for the simulated detector).

c: Constant (c = 7.1272 for the simulated detector), d: Constant (d = 4.1101 for the simulated detector).

e: Constant (e = −0.52234 for the simulated detector), f: Constant (f = −5.8425 for the simulated detector).

The gamma peaks whose energy overlaps with uranium's characteristic X-ray are 92.38 keV (^{234}Th, K_α), 92.80 keV (^{234}Th, K_α), and 112.8 keV (^{234}Th, K_β). The net relative count of the gamma peaks was calculated using equation (3). This research then

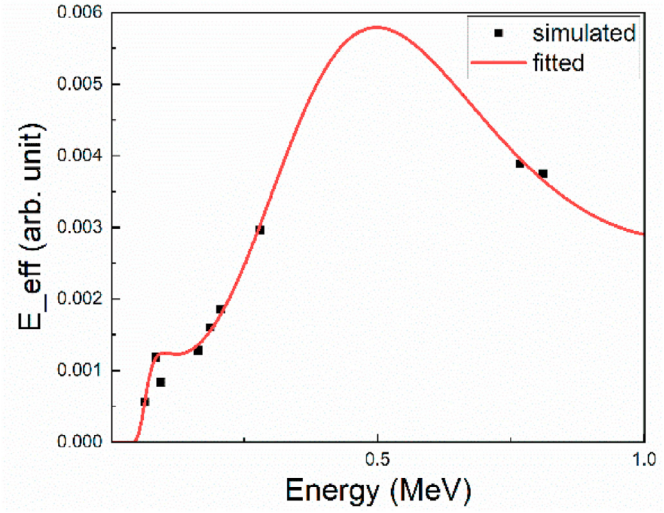

Fig. 5. Energy efficiency curve (simulated and fitted).

calculated the net relative count of K_α and K_β X-rays. Since the simulation results are the averaged results for a single photon, the total gamma photon emission rate was multiplied by the net relative X-ray counts (c_α and c_β). The described simulation and calculation process were performed for 28 UO_2 pellets. Table 5 summarizes the simulation and calculation results for all the pellets.

Equation (6) was then modified into equation (10) using a reference pellet with given ^{235}U enrichment and U concentration. This research defined a reference as a UO_2 pellet whose U concentration and ^{235}U enrichment are 88.15% (0 wt% Gd_2O_3) and 4.5 wt%.

$$\frac{C_{\alpha/\beta,ROI}(w,f_U)}{C_{\alpha/\beta,ROI}\left(w_{ref},f_{ref}\right)} = \frac{\left(Af_U^2 + Bf_U + C\right)}{\left(Af_{ref}^2 + Bf_{ref} + C\right)} \frac{\left(Dw^2 + Ew + F\right)}{\left(Dw_{ref}^2 + Ew_{ref} + F\right)} \tag{10}$$

where.

$C_{\alpha/\beta,ROI}(w, f_U)$: Net K_α and K_β X-ray counts of a target pellet (counts/pellet/sec).

$C_{\alpha/\beta,ROI}(w_{ref}, f_{ref})$: Net K_α and K_β X-ray counts of a reference pellet (counts/pellet/sec).

f_U: U concentration of a target pellet.

f_{ref}: U concentration of a reference pellet.

w: Enrichment of a target pellet (^{235}U wt%), w_{ref}: Enrichment of a reference pellet (^{235}U wt%).

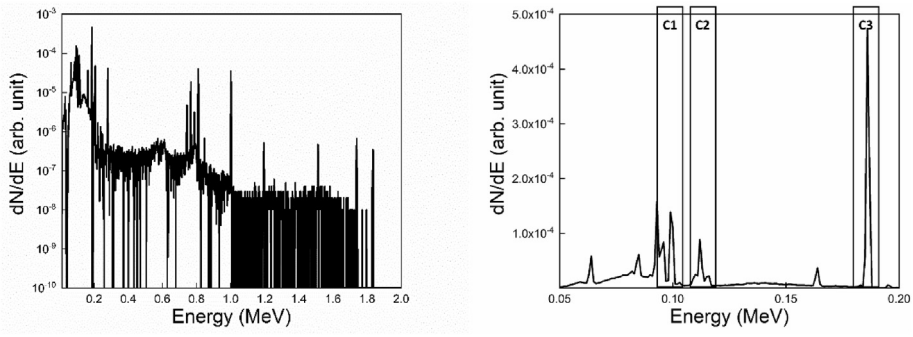

Fig. 4. Energy spectrum of a pellet (88.15% U concentration, 4.5 wt% ^{235}U enrichment), (left: 10–2,000 keV, right: 50–200 keV), (C_1 : 5.56 × 10^{-4}, C_2 : 1.05 × 10^{-4}, C_3 : 7.15 × 10^{-4}).

Table 5
Simulated net K_α and K_β X-ray counts of UO_2 pellets.

Simulated net count of uranium's characteristic X-ray (counts/pellet/sec)					
X-ray types	Enrichment (wt%^{235}U)	U factor (%) (Gd_2O_3 fraction (wt%))			
		88.15 (0)	84.62 (4)	82.86 (6)	81.09 (8)
K_α	**1.5**	3.1247	2.6508	2.4657	2.2444
	2.0	3.9138	3.3884	3.1255	2.8745
	2.5	4.7708	4.1575	3.8930	3.5944
	3.0	5.6170	4.9460	4.6384	4.3312
	3.5	6.4333	5.6869	5.3725	5.0162
	4.0	7.2898	6.4596	6.0860	5.6515
	4.5	8.2595	7.3579	6.9170	6.4438
K_β	**1.5**	0.8898	0.8144	0.7698	0.7165
	2.0	1.1706	1.0350	1.0137	0.8883
	2.5	1.3469	1.2242	1.1558	1.0889
	3.0	1.4600	1.3272	1.2421	1.1570
	3.5	1.7587	1.5918	1.5008	1.4085
	4.0	1.9522	1.7715	1.6691	1.5704
	4.5	2.1411	1.9418	1.8330	1.7341

Since the effect of each parameter (U concentration and ^{235}U enrichment) is independently applied on the X-ray counts, this research normalized the results of Table 5 with the ^{235}U enrichment $(C_{ROI}(w,f_U)/Avg(C_{ROI}(w)))$ and U concentration $(C_{ROI}(w,f_U)/Avg(C_{ROI}(f_U)))$ of a pellet. The net counts normalized with ^{235}U enrichment were only affected by the U concentration, and the net counts normalized with U concentration were only affected by ^{235}U enrichment. Constants (A-F) in equation (10) were calculated using the normalized net counts with each pellet parameter (^{235}U enrichment and U concentration). Figs. 6 and 7 depict the results of polynomial fitting using the net counts normalized with ^{235}U enrichment and U factor, respectively. The results also calculated the constants (A-F) and the goodness-of-fit (R^2 value) for both K_α and K_β X-rays. Since the goodness-of-fit results between K_α and K_β X-ray counts were consistent, the preference of K_α X-ray was higher than the K_β X-ray for the OUCA method due to its higher counts. Equation (10) then becomes equation (11) using the calculated constants (A-F) and the simulated count of a reference pellet. Since parameters in equation (11) are already known except for the U concentration, the concentration of U in a pellet can be measured on site using gamma spectroscopy.

Since the OUCA method is similar to the enrichment meter method, it can be applied for all homogeneous SNMs with fixed geometry. Future research includes a feasibility demonstration of the OUCA method for other SNMs with different nuclides (Pu, Th), compositions (U_3O_8, UO_3, UF_4, etc.) and physical forms (powder, metal, etc.). Since the scintillator detectors have much higher counts compared to the HPGe detector, future research will demonstrate the feasibility of applying NaI(Tl) and LaBr detectors for the OUCA method. If possible, the OUCA method will be a strong on-site method for SNM concentration measurement. Once the OUCA method is applied to on-site inspection, the IAEA's sampling method can be directly applied to ROK's national inspections.

1.3. Validation experiments

This research also performed validation experiments using an n-type HPGe gamma detector and five UO_2 pellets with similar geometry. The characteristics of target pellets are described in Table 6. The difference in pellet geometry and mass occurred due to the difference in manufacturing process and pellet fragments during storage. The HPGe detector used for validation experiments is the same detector used for simulation. The distance between the pellets and the detector crystal was 8 cm to minimize dead time. The live time for each measurement was 3600 s to satisfy sufficient counts. Since the FWHM of X-ray peaks was about 1 keV, the HPGe detector distinguished X-ray peaks and gamma peaks. As a result, the net count of uranium's K_α X-ray was directly calculated using the Gamma Vision software (see Fig. 8).

Since the OUCA method calculates the U concentration of UO2 pellets with given ^{235}U enrichment, validation experiment calculated U concentrations of the five pellets using the declared enrichments. This research measured the net K_α X-ray count of each

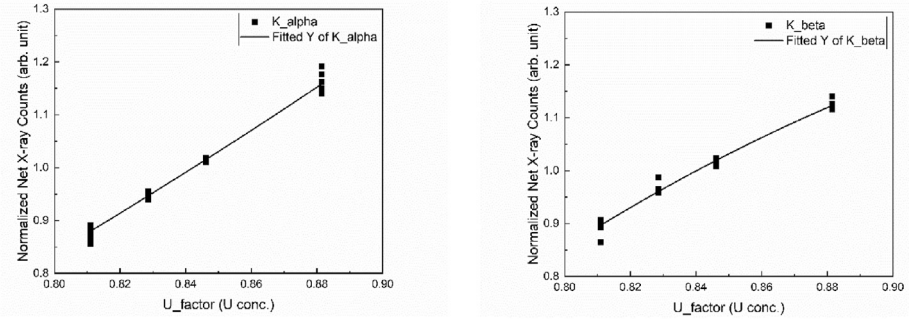

Relative net K_α counts ($R^2 = 0.9863$)
(A_α: 2.7241, B_α: -0.66077, C_α: -0.37589)

Relative net K_β counts ($R^2 = 0.9860$)
(A_β: -7.6683, B_β: 16.1880, C_β: -7.1878)

Fig. 6. Normalized X-ray counts with the same ^{235}U enrichment.

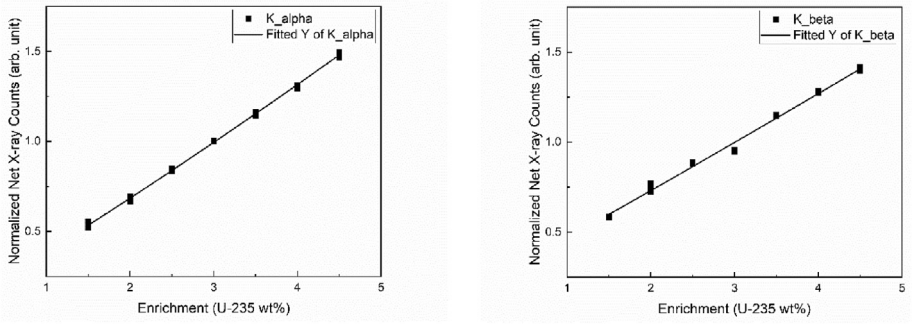

Fig. 7. Normalized X-ray counts with the same U concentration.

$$C_{\alpha,ROI}(w,f_U) = 2.3320 \times \left(A_\alpha f_U^2 + B_\alpha f_U + C_\alpha\right)\left(D_\alpha w^2 + E_\alpha w + F_\alpha\right) \tag{11}$$

Table 6
Characteristics of UO_2 pellets used for experiment.

	B002	B003	Ref#3	Ref#4	Ref#7
U conc. (U%)	80.80	82.53	88.15	88.15	88.15
^{235}U enrichment(wt%)	2.199	2.203	1.280	2.340	3.800
Mass (g)	5.215	5.245	5.364	5.360	5.325
Diameter (mm)	8.200	8.200	8.250	8.250	8.200
Height (mm)	9.800	9.800	9.950	9.900	9.800
Density (g/cm^3)	10.08	10.13	10.08	10.13	10.29

pellet. The reference pellet for the experiment was Ref#4 (U concentration 88.145%, ^{235}U enrichment 2.34 wt%). It then normalized the measured counts with U concentration and ^{235}U enrichment. The constants (A-F) of equation (10) were calculated using the normalized counts. This research then calculated the U concentration of pellets using the measured net X-ray counts and declared ^{235}U enrichments. The calculated U concentration and declared U concentration were compared to validate the OUCA method. This research also performed simulations using the same detector and pellets. It compared the experimental results and simulation results.

The difference between the experimental and simulated results are summarized in Table 7. Results indicate experimental and simulated results have higher U concentration difference for some pellets (B002, B003) than the others (Ref#3, Ref#4, Ref#7). This indicates the effect of the geometry and U concentration on the net X-ray count are much more dominant than the effect of ^{235}U enrichment. Since the energy efficiency applied to five pellets was calculated using the geometry of Ref #4, the pellets with different U concentration and geometry have higher difference. The difference and uncertainty for all cases were less than 5%.

This research calculated the efficiency curve of the detector using the manufacturer's information. However, due to the geometry difference between the declared and real detector geometry, the simulated efficiency curve has to be adjusted. The adjustment will be performed by comparing the measurement results of a reference pellet and simulated results using the same computational model.

Fig. 9 depicts the calculated U concentrations of the experimental results and the difference between the declared and calculated results. The maximum difference between the declared and calculated U concentration was 1.5% for Ref#7 (U concentration 88.145%, ^{235}U enrichment 2.34 wt%). The maximum relative uncertainty of the calculated U concentration was 4.4% for Ref#3 (U concentration 88.145%, ^{235}U enrichment 1.28 wt%). The U concentration difference in Table 7 was derived from the mass and geometry inconsistency between the five pellets.

This research classified the pellets into two groups: (1) pellets with similar ^{235}U enrichment and different U concentration (B002, B003, and Ref#4), (2) pellets with the same U concentration and different ^{235}U enrichment (Ref#3 Ref#4, and Ref#7). It then compared the difference and uncertainty of calculated U concentrations between the two groups to evaluate the integrity of two polynomials in equation (10) (U concentration and ^{235}U enrichment). The results indicated that group (2) had a larger difference and uncertainty compared to group (1), which means the integrity of $D_\alpha w^2 + E_\alpha w + F_\alpha$ is not solid compared to $A_\alpha f_U^2 + B_\alpha f_U + C_\alpha$. The results indicated that the ^{235}U enrichment fitting of equation (10) can only be applied for UO_2 pellets which have similar ^{235}U enrichment to a reference pellet. The results revealed that the OUCA method requires a number of reference pellets with different ^{235}U enrichments to increase its accuracy.

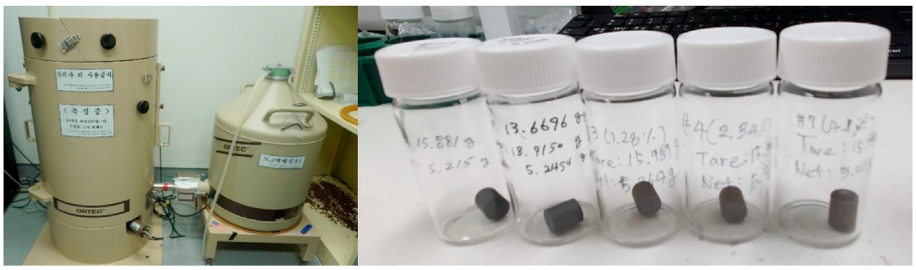

Fig. 8. HPGe gamma detector (left) and UO_2 pellets (right) for the experiment.

Table 7
Measured counts, calculated U concentrations, and uncertainties of validation experiments.

Target	Declared U Conc. (U%)	Experimental Results		Simulated Results	
		U Conc. (U%) (95% CI)	U Conc. Diff. (%)	U Conc. (U%) (95% CI)	U Conc. Diff. (%)
B002	80.80	80.80 ± 0.8936	4.479×10^{-3}	76.89 ± 3.844	4.839×10^{0}
B003	82.53	82.53 ± 1.415	2.949×10^{-3}	79.13 ± 3.957	4.117×10^{0}
Ref#3	88.15	87.82 ± 7.612	3.725×10^{-1}	88.46 ± 4.423	1.451×10^{0}
Ref#4	88.15	88.91 ± 1.951	8.654×10^{-1}	88.15 ± 4.408	$\leq 1.000 \times 10^{-3}$
Ref#7	88.15	86.87 ± 4.444	1.451×10^{0}	88.35 ± 4.417	2.244×10^{0}

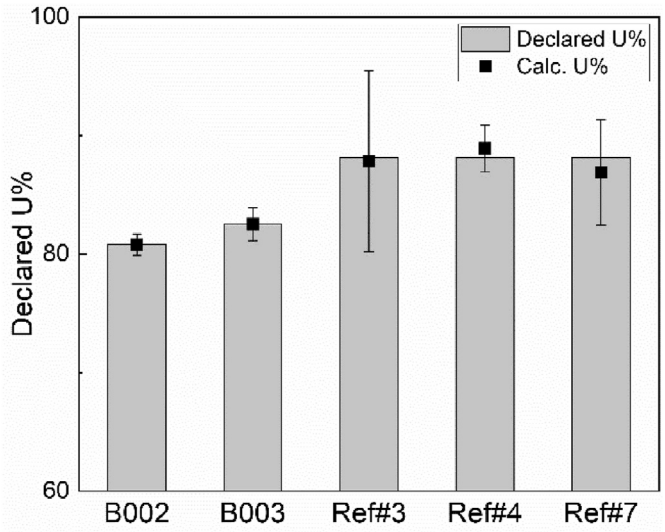

Fig. 9. Results of validation experiments.

The experimental results also demonstrated the feasibility of the OUCA method on UO_2 pellets with similar geometry. However, the results had the limitation that it was for a small number of target pellets, inconsistency between target pellets, and a relatively long detection time. Future experiments will have to consider the limitations above. They need to increase the number of UO_2 pellets with controlled geometry and have different U concentrations and different ^{235}U enrichments to enhance the integrity of the polynomial fitting. The polynomial fitting also has to be performed using a number of reference UO_2 pellets with different ^{235}U enrichments. Since an on-site measurement environment does not allow 3600 s of measurement time, it also has to reduce the measurement time. Future studies will reduce measurement time by reducing the source-detector distance or using scintillator detectors.

2. Conclusion

As the IAEA implements integrated safeguards (IS) and a state level approach (SLA) to its member states, national inspection becomes more important. Due to the domestic notification, the Republic of Korea (ROK) has to verify the special nuclear material (SNM) concentration as well as the total amount of SNM for partial defect verification. However, conventional methods have limitations for on-site SNM concentration analysis, since DA based methods cannot be applied on site while NDA based methods are appropriate for qualitative analysis.

This research suggested a novel on-site uranium concentration analysis (OUCA) method which analyzes the U concentration of UO_2 pellets using gamma spectroscopy. The OUCA method can be applied on site and does not require an additional burden since gamma spectroscopy is already applied for partial defect verification. The proposed method calculated the U concentration and measured the net count of uranium's K_α X-ray, K_β X-ray and the 185.7 keV gamma peak. Since the ^{235}U enrichment of a target pellet and the gamma emission yield of nuclides are known parameters, the OUCA method can calculate the count of overlapped gamma peaks near the X-ray peaks. The method then calculates the net X-ray counts of a target pellet by subtracting the sum of gamma counts from the net counts. The net K_α and K_β X-ray counts are proportional to ^{235}U enrichment and U concentration if the geometry of target UO_2 pellets is consistent.

With this study, the KINAC demonstrated the feasibility of the OUCA method using the MCNPX code, the HPGe gamma detector, and 28 benchmark cases with seven different ^{235}U enrichments (1.5, 2.0, 2.5, 3.0, 3.5, 4.0, 4.5 wt%) and four different U concentrations (81.093, 82.856, 84.619, 88.145 %U). The simulated net K_α and K_β X-ray counts were normalized with respect to the U concentration and enrichment. The X-ray counts normalized with the U concentration were fitted to a polynomial as a function of ^{235}U enrichment and vice versa. The results confirmed that both net K_α and K_β X-ray counts can be calculated by multiplying two fitted polynomials. If the measurement results of reference UO_2 pellets with different ^{235}U enrichments and U concentrations are given, the OUCA method can calculate the U concentration of a UO_2 pellet with the given enrichment.

This research also performed experiment using an n-type HPGe gamma detector and five UO_2 pellets with different U concentrations and ^{235}U enrichments. The experimental results also demonstrated the feasibility of the OUCA method. However, due to the limited number of pellets, the integrity of polynomial fitting will have to be demonstrated with additional experiments. Future work will include additional experiments using an increased number of pellets with different U concentrations and ^{235}U enrichment.

This research suggested the OUCA method and demonstrated the feasibility of the method. Results of this research confirmed the feasibility of on-site U concentration analysis for UO_2 pellets without any additional burden. The ROK requires a novel "on-site" method to measure the U concentration of UO_2 pellets to satisfy the domestic notification and apply the IAEA's sampling method. However, conventional methods, used for U concentration analysis, are DA based or qualitative methods. The OUCA method can be an option for the ROK to adopt the IAEA's sampling method for national inspection. The OUCA method can also be applied for other SNMs with different nuclides, compositions and physical form. The feasibility of the method for different SNMs will be demonstrated in future studies. The feasibility of applying other detector types will also be demonstrated in the future.

Declaration of competing interest

The authors declare that they have no known competing financial interests or personal relationships that could have appeared to influence the work reported in this paper.

References

[1] International Atomic Energy Agency (IAEA), in: The Structure and Content of Agreements between the Agency and States Required in Connection with the Treaty on the Non-proliferation of Nuclear Weapons, vol. 9, 1972. INFCIRC/153 (corrected).

[2] Korea Institute of Nuclear Non-proliferation and Control (KINAC), Handbook of Nuclear Safeguards, 2019, pp. 112–116. KINAC/INSA-001/2019.

[3] Ministry of Government Legislation (ROK MOLEG), Notification on special nuclear material (n.d.). Retrieved May 29, 2020, from, http://law.go.kr/admRulSc.do?tabMenuId=tab107.

[4] H. Lee, H.Y. Kim, J.Y. Choi, H. Seo, Investigation of optimized sample size of nuclear fuel pellets for national inspection, Transactions of the KNS autumn meeting, Goyang, ROK (2019). October 23-25.

[5] International Atomic Energy Agency (IAEA), Safeguards Techniques and Equipment 2003 Edition, 2003, pp. 27–30. International Nuclear Verification Series No. 1, IAEA/NVS/1(Rev.).

[6] S.C. Shon, et al., Comparative analysis for the determination of nuclear materials in spent fuels by electrochemical method, Transactions of the KNS Spring meeting, Jeju, ROK (2001). May 24-25,.

[7] K. Zhao, et al., International Target Values 2010 for Measurement Uncertainties in Safeguarding Nuclear Materials, vol. 48, IAEA ESRADA BULLETIN, 2012, pp. 14–20.

[8] S. Ahn, et al., Development of Reliability Improvement Plan for Thermogravimetric Analysis for the Measurement of UO_2 Stoichiometry, 2018, pp. 3–4. KINAC/CR-005/2018.

[9] K. Ollila, K. Lindqvist, Air-oxidation Tests with Gd-Doped UO_2: Preliminary Dissolution Experiments with Pre-oxidized Gd-Doped UO_{2+x}, 2003, pp. 11–16. Posiva 2003-08.

[10] S. Dhara, S.S. Kumar, N.L. Mirsa, Betterment in EDXRF analytical results for compositional characterization of mixed uranium thorium oxide samples with bead specimens compared with pressed pellet specimens, X Ray Spectrom. 45 (2016) 268–273.

[11] D.B. Pelowitz, MCNPX^{TM} User's Manual Version 2.7.0, 2011, pp. 5–139. LA-CP-11-00430.

[12] S.M. Bowman, I.C. Gauld, OrigenArp Primer, How to Perform Isotopic Depletion and Decay Calculations with SCALE/ORIGEN, 2010, pp. 21–36. ORNL/TM-2010/43.

[13] Korea Atomic Energy Research Institute (KAERI), Table of gamma rays, Retrieved March 10, 2020, from, http://atom.kaeri.re.kr:8080/gamrays.html.

[14] M. Caccia, A. Ebolese, M. Maspero, R. Santoro, Background removal procedure based on SNIP algorithm for gamma ray spectroscopy with the CAEN Educational Kit, Educational Note 2 (2017) ED3163.